J|A|C|S
ARTICLES

Published on Web 12/03/2010

Structure, Interactions, and Antibacterial Activities of MSI-594 Derived Mutant Peptide MSI-594F5A in Lipopolysaccharide Micelles: Role of the Helical Hairpin Conformation in Outer-Membrane Permeabilization

Prerna N Domadia,[†] Anirban Bhunia,[†] Ayyalusamy Ramamoorthy,*[,‡] and Surajit Bhattacharjya*[,†]

School of Biological Sciences, Nanyang Technological University, 60 Nanyang Drive, Singapore-637551 and Department of Chemistry and Biophysics, University of Michigan, Ann Arbor, Michigan 48109-1055, United States United States of America

Received September 15, 2010; E-mail: surajit@ntu.edu.sg; ramamoor@umich.edu

Abstract: Lipopolysaccharide (LPS) provides a well-organized permeability barrier at the outer membrane of Gram-negative bacteria. Host defense cationic antimicrobial peptides (AMPs) need to disrupt the outer membrane before gaining access to the inner cytoplasmic membrane or intracellular targets. Several AMPs are largely inactive against Gram-negative pathogens due to the restricted permeation through the LPS layer of the outer membrane. MSI-594 (GIGKFLKKAKKGIGAVLKVLTTG) is a highly active AMP with a broad-spectrum of activities against bacteria, fungi, and virus. In the context of LPS, MSI-594 assumes a hairpin helical structure dictated by packing interactions between two helical segments. Residue Phe5 of MSI-594 has been found to be engaged in important interhelical interactions. In order to understand plausible structural and functional inter-relationship of the helical hairpin structure of MSI-594 with outer membrane permeabilization, a mutant peptide, termed MSI-594F5A, containing a replacement of Phe5 with Ala has been prepared. We have compared antibacterial activities, outer and inner membrane permeabilizations, LPS binding affinity, perturbation of LPS micelles structures by MSI-594 and MSI-594F5A peptides. Our results demonstrated that the MSI-594F5A has lower activities against Gram-negative bacteria, due to limited permeabilization through the LPS layer, however, retains Gram-positive activity, akin to MSI-594. The atomic-resolution structure of MSI-594F5A has been determined in LPS micelles by NMR spectroscopy showing an amphipathic curved helix without any packing interactions. The 3D structures, interactions, and activities of MSI-594 and its mutant MSI-594F5A in LPS provide important mechanistic insights toward the requirements of LPS specific conformations and outer membrane permeabilization by broad-spectrum antimicrobial peptides.

Introduction

The rapid evolution of conventional antibiotic resistance bacterial species has emerged as a major challenge toward human health.[1,2] Several Gram-negative and Gram-positive bacterial isolates, termed as multi-drug resistant (MDR) strains, are now known to acquire resistance against a number of antibiotics.[3−5] Among these MDR strains, as realized, the Gram-negative species e.g., *P. aeruginosa*, *A. baumannii*, and *K. pneumonia* have created major threat due to lack of active drug candidates.[5] The elevated degree of protection against these antibiotics of Gram-negative organisms are manifested by the permeability barrier imposed by the outer membrane.[5−8] Thus, new antibiotics with different modes of actions are highly required to combat infectious diseases. The host defense cationic antimicrobial peptides (AMPs), evolutionarily preserved elements of the innate immune systems, have been recognized as viable candidates for development of new generation of novel antibiotics.[9−11] AMPs serve the first line of defense against invading pathogens with a broad-spectrum of activities toward bacteria, viruses, fungi.[9−11] Some AMPs even contain antiparasitic activities and can exhibit selective toxicity against cancer cells.[12−14] In higher organisms including humans, AMPs are related to the plausible stimulation and modulation of adaptive immunities.[15,16] Bactericidal activities of most of the cationic AMPs stem from their ability to disrupt the integrity of

[†] School of Biological Sciences, Nanyang Technological University.
[‡] Department of Chemistry and Biophysics, University of Michigan.

(1) Verhoef, J. *Adv. Exp. Med. Biol.* **2003**, *531*, 301–313.
(2) Levy, S. B.; Marshall, B. *Nat. Med. (suppl.)* **2004**, *10*, S122–S129.
(3) Walsh, F. M.; Amyes, S. G. B. *Curr. Opin. Microbiol.* **2004**, *7*, 439–444.
(4) Weinstein, R. A. *Emerg. Infect. Dis.* **2001**, *7*, 188–192.
(5) Taubes, G. *Science* **2008**, *321*, 356–361.
(6) Nikaido, H. *Science* **1994**, *264*, 382–388.
(7) Nikaido, H. *Microbiol. Mol. Biol. Rev.* **2003**, *67*, 593–656.
(8) Delcour, A. H. *Biochim. Biophys. Acta* **2009**, *1794*, 808–816.
(9) Hancock, R. E. W. *Lancet* **1997**, *349*, 418–422.
(10) Zasloff, M. *Nature* **2002**, *415*, 389–395.
(11) Brogden, K. A. *Nat. Rev. Microbiol.* **2005**, *3*, 238–250.
(12) Hoskin, D. W.; Ramamoorthy, A. *Biochim. Biophys. Acta* **2008**, *1778*, 357–375.
(13) Papo, N.; Shai, Y. *Cell. Mol. Life Sci.* **2005**, *62*, 784–790.
(14) Mor, A. *FEBS J.* **2009**, *276*, 6474–6482.
(15) Dhople, V.; Krukemeyer, A.; Ramamoorthy, A. *Biochim. Biophys. Acta* **2006**, *1758*, 1499–1512.

membrane structures.[17−21] The amphipathicity characteristics, rendered by cationic and hydrophobic sequence features, of AMPs allow them to bind cellular membranes of microorganisms.[17−21] Peptide mediated cell lysis occurs due to the insertion of AMPs into cytosolic membranes following one or several mechanisms, e.g., barrel stave, toroidal pore, or carpeting.[18−20] Consequently, structure−activity correlation studies of AMPs are mostly carried out either in negatively charged phospholipids or in a mixture of zwitterionic and negatively charged phospholipids mimicking cytosolic membranes of bacteria.[17−21] However, AMPs should interact with the cell wall or outer membrane components of bacteria before gaining access to the plasma membranes.[22−24] The highly anionic lipopolysaccharide (LPS) layer of the outer leaflet of the outer membrane of Gram-negative bacteria serves as a permeability barrier not only against antibiotics but also for antimicrobial peptides and host defense proteins.[8,25,26] Higher peptide concentrations are often required to inhibit growth of Gram-negative organisms as compared to Gram-positive ones.[27,28] Some AMPs are found to be rather inactive against Gram-negative strains.[27,28] Recent studies demonstrated temporins, a group of short antimicrobial peptides from European frogs, showed activities only against Gram-positive bacteria.[29,30] Similar observations are also made by Shai and co-workers, whereby LPS of the outer membrane was involved in inactivation of a set of designed cationic amphipathic Lys/Leu rich helical peptides.[31] In LPS, these AMPs transition into aggregated states preventing translocation through the outer membrane.[29−31] In order to achieve a high activity, AMPs have to overcome the LPS permeability barrier of the outer membrane. Amphiphilic LPS is composed of three distinct domains: a well conserved lipid A moiety made of by polyacylated glucosamine-based bis-phospholipid, a core oligosaccharide, and a highly variable polysaccharide or the O-antigen.[24,32] It has been proposed that AMPs may disrupt the outer membrane via a "self-promoted" uptake mechanism, wherein cationic residues of peptides interact with phosphate groups of LPS after displacing divalent cations.[25,26] However, atomic-resolution structures and interactions of AMPs in LPS lipids would be vital to understand mechanisms of action and for further design of potent antibiotic peptides.[22,32−35] Moreover, LPS or endotoxin, under certain circumstances, may cause overstimulation of innate systems causative of fatal septic shock syndromes in human.[36,37] AMPs with LPS binding and neutralizing ability would provide starting point for the development of antiendotoxic drugs.[38,39]

A series of highly active broad-spectrum AMPs, termed MSI, were obtained from SAR studies of magainin, PGLa, and melittin.[40−42] Among these peptides, MSI-78 (also known as pexiganan) and MSI-594 contain a broad-spectrum of activities against a variety of pathogens including drug resistance bacteria, both Gram-negative and Gram-positive, fungi, and virus.[40−42] The magainin variant, MSI-78 holds promising prospective in the clinical phase III drug trials for applications against bacterial infections,[41] while MSI-594 shows antiviral activity against HSV type I.[43] Specifically, MSI-594 is a lysine-rich, synthetic hybrid of MSI-78 (residues 1 to 11) and melittin (residues 1 to 13), originally designed and synthesized by Genaera Corporation.[41] Apart from being nonhemolytic, MSI-594 is found to be more active than other AMPs like melittin, magainin, omiganan, indolicidin, dermaseptin, and cecropin.[41] Solid-state NMR, DSC, and ^{31}P NMR described a carpet mechanism for this membrane-active peptide, where the helical axis lays nearly parallel to the lipid bilayer surface.[44,45] Further studies with NMR spectroscopy revealed a straight monomeric helical structure for DPC micelle bound MSI-594 peptide.[46] Recently, we have determined the 3-D structure of MSI-594 in LPS micelles using NMR spectroscopy.[33] MSI-594 adopts amphipathic helical hairpin structure or helix-turn-helix in its LPS bound complex, where the aromatic ring of residue Phe5 and the side chain methyl groups of residues Ile2, Ile13, Leu17, and Leu20 are in close contact with LPS.[33] MSI-594 also possesses a surface orientation in LPS micelles.[33] We have hypothesized that the compact helical structure of MSI-594 may be a prerequisite for the translocation across the LPS membrane. In this work, the plausible role of such an LPS-specific conformation of MSI-594 has been examined using a mutated variant of MSI-594 or MSI-594F5A, whereby the Phe5 residue was mutated to Ala. Such replacement may reduce or abolish the interhelical packing interactions observed in LPS micelles affecting outer membrane permeabilization and antibacterial activities. Our functional studies have revealed that MSI-594F5A peptide shows a markedly reduced activity against Gram-negative organisms with very little change of activity, in comparison to MSI-594, against Gram-positive bacteria. There was a dramatic decrease in permeabilization of the outer membrane of Gram-negative cells by MSI-594F5A, as suggested

(16) Brown, K. L.; Hancock, R. E. *Curr. Opin. Immunol.* **2006**, *18*, 24–30.
(17) Epand, R. M.; Vogel, H. J. *Biochim. Biophys. Acta* **1999**, *1462*, 11–28.
(18) Matsuzaki, K. *Biochim. Biophys. Acta* **1998**, *1376*, 391–400.
(19) Haney, E. F.; Hunter, H. N.; Matsuzaki, K.; Vogel, H. J. *Biochim. Biophys. Acta* **2009**, *1788*, 1639–1655.
(20) Shai, Y. *Biochim. Biophys. Acta* **1999**, *1462*, 55–70.
(21) Ramamoorthy, A. *Solid State Nucl. Magn. Reson.* **2009**, *35*, 201–207.
(22) Bhattacharjya, S.; Ramamoorthy, A. *FEBS J.* **2009**, *276*, 6465–6473.
(23) Snyder, D. S.; McIntosh, T. J. *Biochemistry* **2000**, *39*, 11777–11787.
(24) Ding, L.; Yang, L.; Weiss, T. M.; Waring, A. J.; Lehrer, R. I.; Huang, H. W. *Biochemistry* **2003**, *42*, 12251–12259.
(25) Hancock, R. E. W. *Annu. Rev. Microbiol.* **1984**, *38*, 237–264.
(26) Hancock, R. E. W.; Chapple, D. S. *Antimicrob. Agents Chemother.* **1999**, *43*, 1317–23.
(27) Steiner, H.; Hultmark, D.; Engstrom, A.; Bennich, H.; Boman, H. G. *Nature* **1981**, *292*, 246–248.
(28) Dante, M.; Wieprecht, T. *Biochim. Biophys. Acta* **1999**, *1462*, 71–87.
(29) Rosenfeld, Y.; Barra, D.; Simmaco, M.; Shai, Y.; Mangoni, M. L. *J. Biol. Chem.* **2006**, *281*, 28565–28574.
(30) Mangoni, M. L.; Shai, Y. *Biochim. Biophys. Acta* **2009**, *1788*, 1610–1619.
(31) Papo, N.; Shai, Y. *J. Biol. Chem.* **2005**, *280*, 10378–10387.
(32) Bhattacharjya, S. *Curr. Med. Chem.* **2010**, *17*, 3080–3093.
(33) Bhunia, A.; Ramamoorthy, A.; Bhattacharjya, S. *Chemistry* **2009**, *15*, 2036–2040.
(34) Japelj, B.; Pristovsek, P.; Majerle, A.; Jerala, R. *J. Biol. Chem.* **2005**, *280*, 16955–16961.
(35) Bhunia, A.; Mohanram, H.; Domadia, P. N.; Torres, J.; Bhattacharjya, S. *J. Biol. Chem.* **2009**, *284*, 21991–22004.
(36) Cohen, J. *Nature* **2002**, *420*, 885–891.
(37) Martin, G. S.; Mannino, D. M.; Eaton, S.; Moss, M. *N. Engl. J. Med.* **2003**, *348*, 1546–1554.
(38) Scott, M. G.; Vreugdenhil, A. C.; Buurman, W. A.; Hancock, R. E.; Gold, M. R. *J. Immunol.* **2000**, *164*, 549–553.
(39) Jerala, R.; Porro, M. *Curr. Top. Med. Chem.* **2004**, *4*, 1173–1184.
(40) Lamb, H. M.; Wiseman, L. R. *Drugs* **1998**, *56*, 1047–1052.
(41) Gottler, L. M.; Ramamoorthy, A. *Biochim. Biophys. Acta* **2009**, *1788*, 1680–1686.
(42) Maloy, W. L.; Kari, U. P. *Biopolymers* **1995**, *37*, 105–122.
(43) Egal, M.; Conrad, M.; MacDonald, D. L.; Maloy, W. L.; Motley, M.; Genco, C. A. *Int. J. Antimicrob. Agents* **1999**, *13*, 57–60.
(44) Ramamoorthy, A.; Thennarasu, S.; Lee, D. K.; Tan, A.; Maloy, L. *Biophys. J.* **2006**, *91*, 206–216.
(45) Hallock, K. J.; Lee, D. K.; Ramamoorthy, A. *Biophys. J.* **2003**, *84*, 3052–3060.
(46) Porcelli, F.; Buck-Koehntop, B. A.; Thennarasu, S.; Ramamoorthy, A.; Veglia, G. *Biochemistry* **2006**, *45*, 5793–5799.

from lower uptake of hydrophobic dyes. By contrast, release of calcein from 3:1 POPC/POPG liposome and cytoplasmic membrane depolarization were found to occur in a similar fashion for the native and mutant MSI peptides. LPS binding affinity has been estimated for MSI-594 and MSI-594F5A using isothermal titration calorimetry. The mutant variant MSI-594F5A showed a marked reduction in binding to LPS micelles. The ability of MSI peptides to perturb LPS micelles was examined by dynamic light scattering and FITC fluorescence of LPS. The native peptide MSI-594 demonstrated greater perturbations to LPS micelles in comparison to MSI594F5A. As CD spectroscopy delineated helical structure for both peptides in LPS micelles, an ensemble of 3-D structures of LPS-bound mutant MSI-594F5A has been determined by NMR. In the context of LPS, MSI-594F5A assumes a curved amphipathic helical structure without any long-range packing interactions. The outer face of the helix is highly cationic placing all of the six Lys residues, whereas the inner face is made by nonpolar amino acids. Collectively, these results provide important insights regarding specific structural requirements of AMPs in the context of LPS or outer membranes to achieve a broad-spectrum of activities.

Experimental Section

LPS of *E. coli* 0111:B4 and fluorescein isothiocyanate conjugated LPS from *E. coli* 055:B5; 1-*N*-phenylnaphthylamine (NPN), 8-anilinonapthalene-1-sulfonic acid (ANS) were obtained from Sigma Aldrich. ATCC bacterial strains were purchased from the American Type Culture Collection (Rockville, MD). 1-Palmitoyl-2-oleyl-*sn*-glycero-3-phosphocholine (POPC), 1-palmitoyl-2-oleyl-*sn*-glycero-3-phoshoglycerol (POPG) were from Avanti Polar Lipids, Alabaster, AL. Calcein and 3,3′-dipropylthiadicarbocyanine iodide (DiSC3−5) were from Fluka BioChemika. MSI-594 was synthesized as described in our earlier publications[44,45] and MSI-594F5A was prepared and purified by Genscript.

Assay for 1-*N*-phenylnaphthylamine (NPN) Dye Uptake. Overnight culture of *E. coli* BL21 (DE3) cells were grown in Luria−Bertani broth to midlog phase (OD_{600} of 0.35), centrifuged at 3000 $\times g$ for 10 min at 25 °C, washed twice, and resuspended into 5 mM sodium HEPES buffer, pH 7.2 containing 5 mM glucose, 5 mM NaN_3 to a final $OD_{600} \approx 0.5$. Hydrophobic fluorescent dye 1-*N*-phenylnaphthylamine (NPN),[47] at a concentration of 10 μM (prepared in acetone) was added to 500 μL of the resuspended cells and allowed to stabilize. Increasing concentrations, ranging from 0.1 μM to 5 μM, either of native MSI-594 or variant MSI594F5A peptides were added to the treated cells and the increase in NPN fluorescence on account of the outer membrane permeabilization was measured on a Cary Eclipse spectrofluorimeter (Varian, Inc., Palo Alto, CA). NPN fluorescence was measured using an excitation wavelength of 350 nm and emission maximum at 420 nm, employing a bandwidth of 5 nm. The background fluorescence of the free NPN was subtracted from the total fluorescence and plotted against the concentrations of peptides.

Assay for 8-Anilinonapthalene-1-Sulfonic Acid (ANS) Uptake. Overnight culture of *E. coli* BL21 (DE3) cells were grown in Luria−Bertani broth to midlog phase (OD_{600} of 0.35), centrifuged at 3000 g for 10 min at 25 °C, washed and resuspended into 10 mM Tris-HCl (pH 7.4), 150 mM NaCl buffer to a final OD_{600} of 0.5. Fluorescent dye 8-anilinonapthalene-1-sulfonic acid (ANS) at a concentration of 4 μM was added to the above cells, followed by subsequent additions of increasing concentrations of native MSI-594 and variant MSI-594F5A, ranging between 0.5 and 15 μM. An increase of ANS fluorescence intensity on account of outer membrane permeabilization was then measured on a Cary Eclipse spectrofluorimeter (Varian, Inc., Palo Alto, CA) using an excitation wavelength of 350 nm and emission at 500 nm, employing a bandwidth of 5 nm.[48]

Assay for Membrane Depolarization. Overnight stationary-phase Gram-negative *E. coli* BL21 (DE3) cells were subcultured into Luria−Bertani broth for 2−3 h at 37 °C to obtain midlogarithmic phase cells, centrifuged at 2500 $\times g$ for 10 min at 25 °C, washed, and resuspended into respiration buffer (5 mM HEPES, 20 mM glucose, pH 7.4) to obtain a diluted suspension of $OD_{600} \approx 0.05$. Membrane potential-sensitive dye, 3,3′-dipropylthiadicarbocyanine iodide (DiS-C_3-5),[49] 0.2 μM (prepared in DMSO) was added to 500 μL aliquot of the resuspended cells and allowed to stabilize for 1 h. Before the addition of the dye, a final concentration either of 0.1 mM or 1 mM EDTA was added to each aliquot of resuspended cells in order to allow penetration of the dye through the outer membrane of bacterial cells. Baseline fluorescence was acquired using a Cary Eclipse spectrofluorimeter (Varian, Inc., Palo Alto, CA) by excitation at 622 nm and emission at 670 nm, employing a bandwidth of 5 nm, respectively. Subsequently, increasing concentrations of native MSI-594 and variant MSI-594F5A ranging between 0.1 and 30 μM were added to the stabilized cells and the increase of fluorescence on account of the dequenching of DiS-C_3-5 dye was measured after every 5 min to obtain the maximal depolarization. Percent depolarization was calculated by using $F - F_0/F_m - F_0 \times 100$; where F is the fluorescence intensity 5 min after addition of peptide, F_0 is the initial basal fluorescence intensity, and F_m is the maximum fluorescence intensity for MSI-594 peptide. Percent depolarization was plotted versus increasing peptide concentrations, respectively.

Calcein Leakage Assay. In brief, small unilamellar vesicles were prepared by combining lipids POPC/POPG (in 2:1 chloroform/methanol) in a molar ratio of 3:1 to obtain a combined mass of ~20 mg and dried further to obtain a thin film followed by overnight lyophilization. The dried lipid film was further rehydrated by addition of self-quenching buffered calcein solution (70 mM calcein, 10 mM Tris-HCl, pH 7.4), incubation in water-bath at 40 °C for 1 h and vortexed the lipid suspension to obtain multilamellar vesicles (MLVs). MLV suspensions were further subjected to sonication for 3 min, followed by centrifugation at 14000 rpm for 10 min and extrusion for 21 times in small-volume extrusion apparatus using two stacked polycarbonate filters with 50 nm membrane pores (Avanti Polar Lipids, Alabaster, AL). The calcein entrapped SUVs were separated from the free calcein using gel-filtration based, hydrated, Centri-Sep spin columns and eluting light-orange, iridescent lipid suspensions by spinning at 750 $\times g$ for 2 min. A final concentration of 50 μM of 3:1 POPC/POPG SUVs were suspended into 500 μL of extra-vesicular buffer (10 mM Tris-HCl, 100 mM NaCl, pH 7.4) and its fluorescence intensity was measured on a Cary Eclipse spectrofluorimeter (Varian, Inc., Palo Alto, CA) by excitation at 490 nm and emission at 520 nm, employing a bandwidth of 1.5 nm. After the stabilization of calcein fluorescence, increasing concentrations of native MSI-594 and variant MSI-594F5A, ranging between 1 and 30 μM were added to above SUVs aliquots and the increase in fluorescence intensity on account of the dequenching of calcein dye was measured after every 5 min to obtain the maximal leakage. A 5-μL portion of 10% (v/v) aqueous Triton X-100 was employed to get the maximal fluorescence intensity. Percent leakage was calculated by using $F - F_0/F_T - F_0 \times 100$; where F is the fluorescence intensity 5 min after addition of peptide, F_0 is the initial basal fluorescence, and F_T is the total fluorescence (after Triton X-100 addition).

Antibacterial Susceptibility Assay. The antibacterial susceptibility assays for antimicrobial peptides were conducted following procedure previously been used.[50] Briefly, 1 mL of stationary phase cultures of the test organisms namely *Escherichia coli* DH5α, *Bacillus subtilis*, *Pseudomonas aeruginosa* ATCC 27853, *Staphy-*

(47) Loh, B.; Grant, C.; Hancock, R. E. W. *Antimicrob. Agents Chemother.* **1984**, *26*, 546–551.
(48) Slavik, J. *Biochim. Biophys. Acta* **1982**, *694*, 1–25.
(49) Letellier, L.; Shechter, E. *Eur. J. Biochem.* **1979**, *102*, 441–447.

lococcus aureus ATCC 25923, *Klebsiella pneumoniae* ATCC 13883, *Salmonella enteritis* ATCC 14028, and *Enterobacter fecalis* ATCC 29212 were sub cultured into fresh Mueller-Hinton broth for 2−4 h at 37 °C to obtain midlogarithmic phase cells. The bacterial cells were centrifuged at 4000 $\times g$ for 5 min, washed by repeated centrifugation and resuspended in 10 mM sodium phosphate buffer, pH 7.2 and diluted 10^5 fold to obtain a cell density, $A_{600} \approx 0.01$. 50 μL of above bacterial suspensions were incubated in a sterile 96-well microtiter polypropylene plate along with 50 μL final volume of the native MSI-594 and variants MSI-594F5A or controls in each well. The test range for two peptides was between 0.25 to 250 μM. Positive (Polymyxin B sulfate) and negative (assay buffer) controls were also tested. The reaction mixture was incubated for 3 h at 37 °C; thereafter, it was plated onto Mueller Hinton agar plates and incubated for 24 h at 37 °C to estimate minimal inhibitory concentration (MIC) values.

Circular Dichroism (CD) Spectroscopy. Secondary structure was determined for the native MSI-594 and mutant MSI-594F5A peptides by far UV CD method. Peptides were dissolved at 25 μM in a 10 mM sodium phosphate buffer at pH 5.0, either in the absence and presence of 50 μM LPS from *E. coli* 0111:B4. CD data were collected using a Chirascan spectropolarimeter (Applied Photophysics Ltd., UK). The far-UV steady state CD spectra were scanned over the range of 190−240 nm in a 0.01 cm path length sandwich quartz cuvette (Hellma), with an averaging of three scans. Baseline scan was obtained using the same parameters on buffer alone and was subtracted from the scan of peptides. The corrected data obtained in millidegree (θ) were converted to molar ellipticity in deg cm^2 dmol^{-1}; using the Chirascan version 1.2 (Applied Photophysics) provided by the manufacturer.

Isothermal Titration Calorimetry (ITC) Experiments. The energetics of the binding interactions for native MSI-594 and MSI-594F5A variant with LPS were analyzed. All ITC experiments were performed on a MicroCal iTC200 micro calorimeter (MicroCal, Northampton, UK). Peptides and LPS samples were prepared in 10 mM sodium phosphate buffer, pH 6.0. All samples were filtered and degassed. Prior to titration, LPS solution was vortexed for 15 min, heated at 60 °C for 5 min, and sonicated for 2 min. The molecular mass for *E. coli* 0111:B4 LPS was considered to be 10 KDa.[51] A typical titration involved 15 injections of 1 mM peptides (0.4 μL per injection, at an interval of 240 s) into the reaction cell having a volume of 200 μL containing 50 μM LPS. The reaction cell was stirred continuously at 350 rpm. The high feedback mode/gain was selected. The titrations were continued until saturation was achieved at 293 K. Raw data were corrected for the heat of dilution of peptides in buffer. All of the binding isotherms were fitted using Origin v7.0 (MicroCal), assuming a single-site binding model.

Dynamic Light Scattering (DLS) Experiments. Dynamic light scattering experiments carried out on Malvern Zetasizer Nano ZS (Malvern, UK) equipped with a He−Ne laser ($\lambda = 635$ nm) and a back scattering detection at 173°. LPS micelles, of *E. coli* 0111:B4 strain, at a fixed concentration of 1 μM, prepared in 10 mM sodium phosphate, pH 6.0, either in the absence or in the presence of peptides, at a concentration of 2 μM, were exposed to dynamic light scattering to examine apparent particle size distributions. All samples were filtered, degassed prior to use and measured at 298 K using disposable polystyrene UV cells. Viscosity (0.8924) and refractive index (1.330) of phosphate buffer at 298 K were used for data analysis. The viscosity of 10 mM sodium phosphate buffer was estimated using viscometer accessories available with the instrument. Each value was the average of three independent measurements. Normalized intensity autocorrelation functions were analyzed using the size distribution algorithm for CONTIN method,[52] yielding a distribution of diffusion coefficient (D). The hydrodynamic diameter (d_z, nm) was yielded from the measured diffusion coefficient (D) using Stokes−Einstein equation $d_z = kT/3\pi\eta D$; where k is the Boltzmann constant, T is the absolute temperature, and η is the viscosity of the solvent.

Fluorescence Spectroscopy Studies. The effect of peptides on the LPS disaggregation was analyzed by monitoring the fluorescence of the FITC-labeled LPS in the presence of different concentrations of peptides. In brief, 0.5 μM of FITC conjugated LPS from *E. coli* LPS 055:B5 was excited at 480 nm in 10 mM sodium phosphate, pH 6.0 at 298 K in the absence and presence of native MSI-594 and mutant MSI-594F5A, ranging from 0.1 to 15 μM. Fluorescence emission spectra at 515 nm were recorded using Cary Eclipse fluorescence spectrophotometer (Varian, Inc., Palo Alto, CA, USA), employing bandwidths of 5 nm, respectively.

NMR Experiments. All of the NMR spectra were recorded on a Bruker DRX 600 spectrometer, equipped with actively shielded magnet with a cryo-probe and pulse field gradients. Data acquisition and processing were performed with the Topspin software (BRUKER) running on a Linux workstation. Sequence specific assignments of the MSI-594F5A mutant peptide was achieved from two-dimensional TOCSY (mixing time 80 ms) and NOESY (mixing time 400 ms) spectra, acquired in aqueous solution containing 10% D_2O and at pH 4.5 and 298 K. All chemical shifts were referenced using DSS (2,2-dimethyl-2-silapentane-5-sulfonate sodium salt) as an internal standard and NMR data analysis was carried out using the program SPARKY (Goddard, T. D., and Kneller, D. G., University of California, San Francisco). The interaction of the peptide with LPS was examined by recording a series of one-dimensional proton NMR spectra. A typical NMR sample containing 0.5 mM of peptide was titrated with various concentrations of LPS ranging from 5 to 12 μM at pH 4.5 and 298 K. However, the 2-D tr-NOESY experiments were performed at the molar ratio of [LPS]:[peptide] = 1:20 with three different mixing times; 100, 150, and 200 ms. 2-D NOESY experiments in aqueous solution and tr-NOESY experiments for MSI-594F5A in the presence of LPS were performed with 456 increments in t_1 and 2K data points in t_2 using the WATERGATE[53] procedure for water suppression and States-TPPI[54] for quadrature detection in the t_1 dimension. The spectral width was normally 12 ppm in both dimensions. After 16 dummy scans, 72 scans were recorded per t_1 increment. After zero-filling in t_1, 4K (t_2) $\times$ 1K (t_1) data matrices were obtained.

Determination of LPS-Bound Structure. On the basis of cross-peak intensities from two-dimensional tr-NOESY spectra acquired with a mixing time of 150 ms, the tr-NOEs were categorized qualitatively to strong, medium, and weak, which was then translated to upper bound distance limits to 2.5, 3.5, and 5.0 Å, respectively. The lower bound distance was restricted to 2.0 Å, to avoid van-der-Waals repulsion. The LPS-bound structures were calculated solely based on tr-NOE derived distance calculation and no hydrogen bond constraints were used for structure calculation. However, to limit conformational search the ϕ dihedral angles were restricted between −30° to −120° for all residues except for Gly. DYANA program (version 1.5)[55] was used for NMR derived structure calculation. For refining the NMR derived structure calculation, several rounds of structure calculation were carried out and depending on NOE violations, the distance constraints were adjusted. Out of the 100 structures, 20 lowest energy structures

(50) Wiegand, I.; Hilpert, K.; Hancock, R. E. W. *Nat. Protoc.* **2008**, *3*, 163–175.
(51) Yu, L.; Tan, M.; Ho, B.; Ding, J. L.; Wohland, T. *Anal. Chim. Acta* **2006**, *556*, 216–225.
(52) Provencher, S. W. *Comput. Phys. Commun.* **1982**, *27*, 229–242.
(53) Sklenar, V.; Piotto, M.; Leppik, R.; Saudek, V. *J. Magn. Reson. Ser. A* **1993**, *102*, 241–245.
(54) Marion, D.; Ikura, M.; Tschdin, R.; Bax, A. *J. Magn. Reson.* **1989**, *85*, 393–399.
(55) Guntert, P.; Mumenthaler, C.; Wuthrich, K. *J. Mol. Biol.* **1997**, *273*, 283–298.
(56) Laskowski, R. A.; MacArthur, M. W.; Moss, D. S.; Thornton, J. M. *J. Appl. Crystallogr.* **1993**, *26*, 283–291.

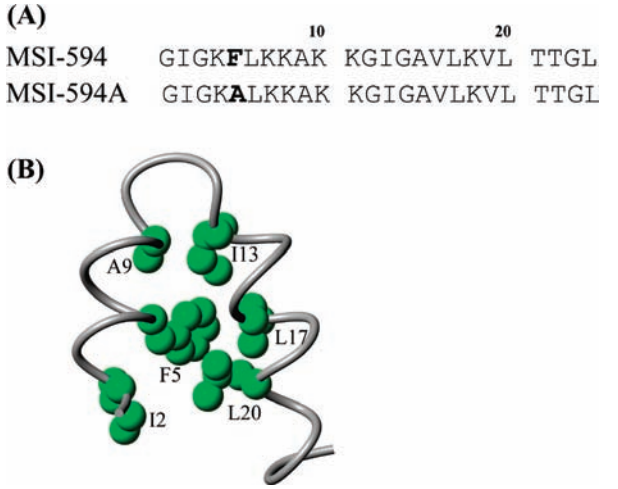

Figure 1. Structure of MSI-594 in LPS micelles. (A) Amino acid sequences of MSI-594 and a mutant peptide MSI-594F5A, replacing residue Phe5 with Ala. (B) Helical hairpin structure of MSI-594 in LPS micelles showing packing interactions between aromatic residue F5 with other aliphatic residues between two helices.

were used for further analysis and the average structure of the 20 ensemble structures were verified using PROCHECK-NMR.[56]

Results

Designing Mutant of MSI-594 and Antimicrobial Activities. The helical hairpin structure of 24-residue MSI-594, derived by NMR spectroscopy, in LPS micelles is characterized by two helices, a short N-terminal helix, residues I2-A9 and a longer C-terminal helix, residues I13-T21, inter connected by a loop, residues K10-G12 (Figure 1). The unique hairpin structure in LPS appears to be stabilized by nonpolar packing interactions whereby the lone aromatic residue F5 of MSI-594 is in close proximity with a number of hydrophobic residues A9, I13, L17, and L20 from two helices (Figure 1). The helical hairpin structure of MSI-594 is highly amphipathic, displaying all of the six positively charged Lys residue at one face of the molecule with an optimum distance separation that may render facile interactions with the phosphate groups of LPS. It is, therefore, likely that the compact structure and geometrical compatibility of LPS/peptide, provided by the orientation of the side chain of basic residues, could be related to an efficient permeabilization of an LPS membrane of Gram-negative bacteria. In order to understand plausible consequences of the hairpin structure of MSI-594 in outer membrane interactions and broad-spectrum of antibacterial activities, the critical residue Phe5 has been mutated to Ala, resulting in an analogue termed MSI-594F5A (Figure 1). The antibacterial activities of MSI-594 and MSI-594F5A have been tested against four Gram-negative and three Gram-positive strains (Table 1). The mutant peptide MSI-594F5A exhibited a marked increase in MIC values against the Gram-negative organisms (Table 1). However, MSI-594 and MSI-594F5A both demonstrated comparable MIC values against Gram-positive strains (Table 1). Surprisingly, a 2-fold higher activity of the mutant peptide was measured against *E. feacalis* (Table 1). Therefore, these results illustrate that the mutation (F5A) has selectively reduced activities of MSI-594F5A peptide against Gram-negative bacteria. Such a decrease in activities may occur due to the inefficient permeabilization of the LPS membrane of Gram-negative strains.

Table 1. MIC Values (in μM) of Native MSI-594 and a Mutant MSI594F5A against Various Gram-Negative and Gram-Positive Bacteria

test strain	MSI-594	MSI-594F5A
E. coli DH5α	1	15
P. aeroginosa ATCC 27853	2	45
K. pneumoniae ATCC 13883	1	8
S. enteritis ATCC 14028	2	8
S. aureus ATCC 25923	2	4
E. feacalis ATCC 29212	64	32
B. subtilis	4	8

Outer Membrane Permeability of Native MSI-594 and Mutant MSI-594F5A. Permeabilization of the outer membrane of *E. coli* cells in the presence of the native MSI-594 and its variant MSI-594F5A was examined on the basis of the fluorescence of 8-anilinonapthalene-1-sulfonic acid (ANS) and 1-*N*-phenylnaphthylamine (NPN) dyes. Hydrophobic ANS and NPN molecules are excluded by cell wall of *E. coli* and thereby emission intensity is quenched in aqueous solution. Disruption of outer membrane integrity by antimicrobial peptides promotes entry of dyes into the hydrophobic environment of perturbed cell membranes resulting an enhanced emission of fluorescence intensity. Figure 2A compares fluorescence of ANS at different concentrations of MSI-594 and MSI-594F5A peptides in presence of *E. coli* cells. The additions of native MSI-594 peptide had caused a dramatic increase in the emission intensity of ANS with a marked blue shift (Figure 2A). By contrast, enhancement of fluorescence intensity of ANS observed for the mutant peptide, MSI-594F5A, was found to be highly limited (Figure 2A). A differential increase in fluorescence intensity of NPN dye had also been detected for MSI-594 and MSI-594F5A (Figure 2B). The fluorescence intensity of NPN shows a larger increase upon inclusions of MSI-594 peptide as compared to the variant one (Figure 2B). These results demonstrate that mutant peptide MSI-594F5A has a markedly reduced efficacy in perturbing integrity of the outer membrane or cell wall in comparison to the native MSI-594.

Depolarization of Cytosolic Membrane of *E. coli* and Liposome Leakage. DiS-C_3-5, a potential sensitive dye, has been used to examine changes in plasma membrane integrity in response to AMPs. The fluorescence of DiS-C3−5 would be quenched in the cytosolic membrane due to self-association, upon gaining access through the cell wall barrier. A dissipation of membrane potential caused by the disruption of membrane integrity will release DiS-C3−5 into solution yielding an increase in fluorescence intensity.[49] The inner membrane depolarization of *E. coli* cells produced by MSI-594 and MSI-594F5A is examined as a function of peptide concentrations and at two different concentrations of EDTA (Figure 3A). EDTA has been known to destabilize the outer membrane through chelating of LPS bound divalent metal ions that enhances the intracellular entry of the DiS-C3−5 dye.[49] At a low concentration (0.1 mM) of EDTA, MSI-594F5A showed a limited fluorescence recovery of DiS-C3−5, by contrast, MSI-594 had exerted a significantly higher level of depolarization of the inner membrane (Figure 3A). The mutant peptide MSI-594F5A appeared to be effective in depolarizing the inner membrane only at higher EDTA concentrations, as revealed by a progressive increase in fluorescence recovery of DiS-C3−5 dye with an increase in peptide concentrations (Figure 3A). The native peptide MSI-594 also demonstrated an increase in inner membrane depolarization in the presence of 1 mM EDTA (Figure 3A). However, as can be seen, the mutant peptide MSI-

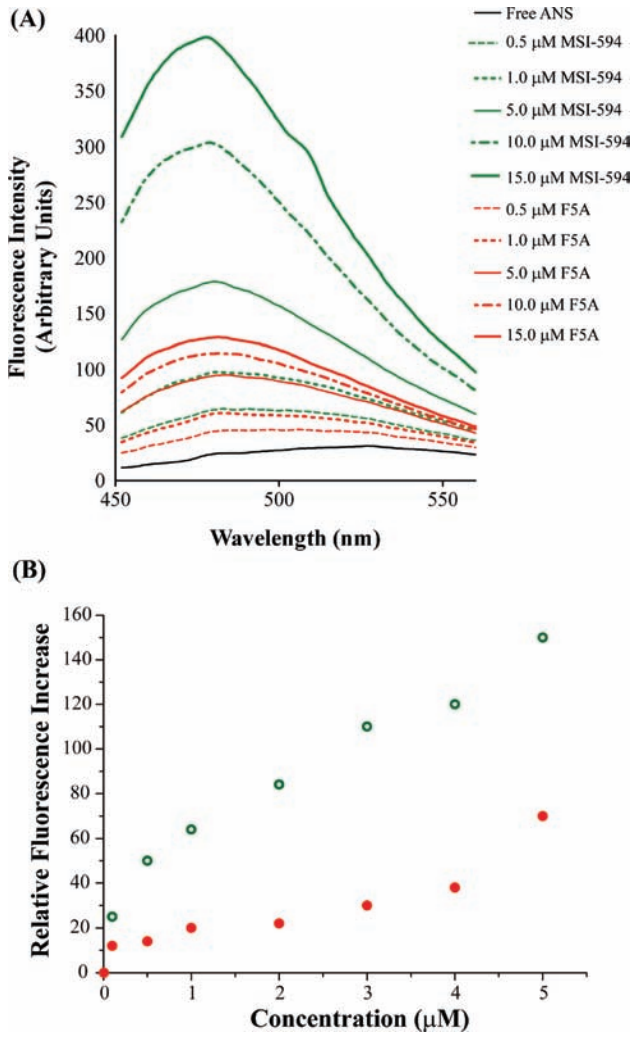

Figure 2. Permeabilization of *E. coli* outer membrane by native MSI-594 and MSI-594F5A. (A) Fluorescence emission spectra of ANS as a function of concentrations of MSI-594 and MSI-594F5A peptides. (B) Plot showing increase in fluorescence intensity of NPN dye in presence of *E. coli* cells with various concentrations of MSI-594 (in green) and MSI-594F5A (in red) peptides. A large increase in intensity of ANS or NPN fluorescence can be seen for MSI-594 peptide as compared to mutant peptide showing that MSI-594F5A has a reduced ability to induce outer membrane permeabilization.

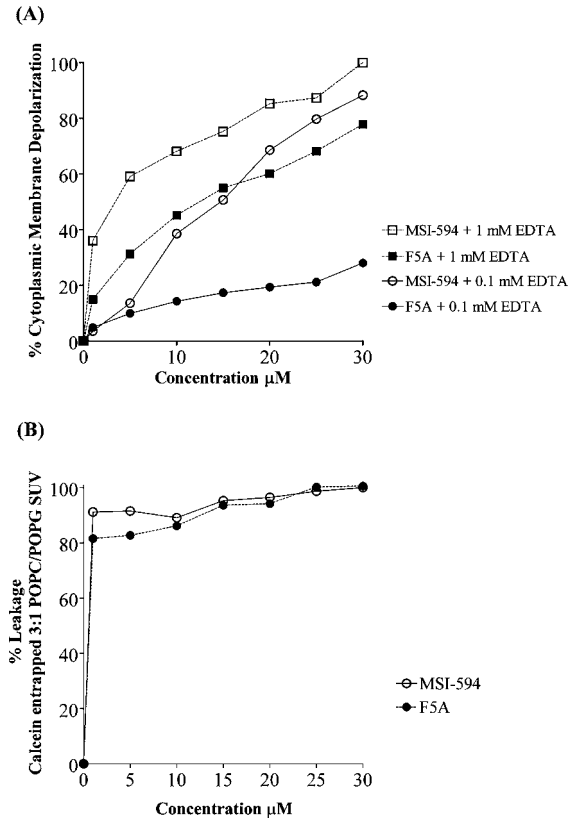

Figure 3. Cytoplasmic membrane depolarization of *E.coli* cells and dye leakage from POPC/POPG vesicles by native MSI-594 and MSI-594F5A peptides. (A) Plot showing membrane depolarization of *E. coli* cells, in the presence of two concentrations of EDTA, as a function of concentrations of MSI-594 and MSI-594F5A peptides. Membrane depolarization was determined from fluorescence dequenching of the potential sensitive dye DiS-C_3-5, at 0.2 μM, in 5 mM HEPES, 20 mM glucose, pH 7.4 using a cell density of $OD_{600} \approx 0.05$ with different concentrations of peptides. (B) Efficacy of calcein dye leakage from small unilamellar vesicles (SUV) composed of 3:1 POPC:POPG lipids as a function of concentrations of MSI-594 and MSI-594F5A peptides.

594F5A delineated a higher degree of dependence toward EDTA concentrations to achieve inner membrane depolarization. These experiments establish once again that the MSI-594F5A has a lower ability to disrupt the integrity of the outer membrane. However, once the outer membrane barrier has been perturbed, as occurred by inclusion of high concentrations of EDTA, MSI-594F5A is effective in disrupting inner membrane integrity. We have further examined the effect of native and mutant MSI-594 peptides to induce dye, calcein, leakage from POPC:POPG (3:1) lipid vesicles as a model of bacterial inner membrane mimic (Figure 3B). Figure 3B shows the release of vesicle entrapped calcein dye upon additions of peptides. In this assay, both peptides MSI-594 and MSI-594F5A show comparable ability to release entrapped calcein from lipid vesicles (Figure 3B). Therefore, it is likely that MSI-594 and the mutant MSI-594F5A may permeabilize the inner membrane of bacteria in a similar fashion.

Binding Energetics of MSI-594 and MSI-594F5A with LPS Micelles. The above-mentioned studies have implicated that a lower activity of MSI-594F5A against Gram-negative bacteria is a consequence of an inability of the peptide to disrupt the outer membrane or LPS layer. In this regard, it is likely that the mutation (F5A) might have altered the binding of MSI-594F5A peptide to LPS lipids. Thereby, we have quantified interactions of MSI-594 and mutant peptide with LPS micelles by use of by isothermal titration calorimetry (ITC) studies. The ITC profiles of native MSI-594 (Figure 4A) and variant MSI-594F5A (Figure 4B) demonstrate discernible differences in saturation behavior while interacting with LPS micelles. The binding induced heat release was found to be saturated at a lower peptide:LPS ratio for MSI-594 (Figure 4A), whereas a higher peptide concentration was required for the mutant MSI-594F5A (Figure 4B). LPS-peptides interactions were observed to be endothermic in nature, as shown by the upward arrangement of titration peaks and the consequent positive integrated heats (Figure 4A,B). For both peptides, a positive change in $T\Delta S$, a positive change in ΔH, and a negative change in ΔG were determined (Table 2). This clearly demonstrates that the binding reactions are driven primarily by a favorable change in entropy and the dominant interactions are hydrophobic in nature. Similar observations were made for the interaction studies of LPS/AMPs

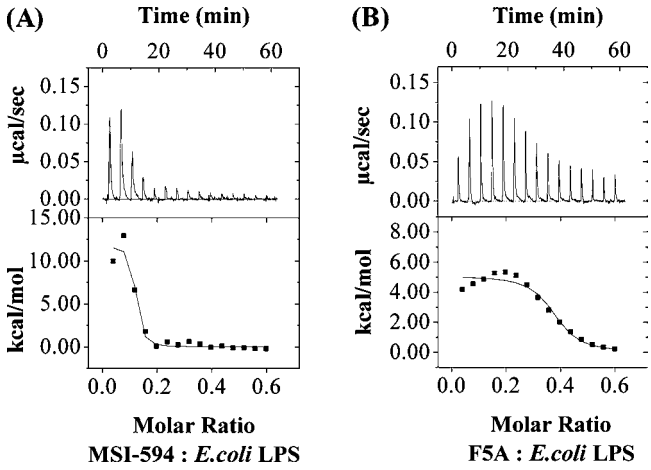

Figure 4. Binding energetics for peptide−LPS interactions by ITC. Calorimetric titration profiles (A and B) for native MSI-594 (A) and MSI-594F5A variant (B). The upper panel shows the titrated peaks plotted as power (in μcal s^{-1}) against time (in min). The lower panel shows the corresponding integrated heats of the interaction. Each 1 mM of peptide titrated against *E. coli* LPS 0111:B4 at a concentration of 0.05 mM in 10 mM sodium phosphate, pH 6.0 at 293K.

Table 2. Thermodynamic Parameters of Interactions between MSI-594 and MSI-594F5A Peptides with LPS Micelles

parameters	MSI-594	MSI-594F5A
K_A (μM^{-1})	13.20	3.10
ΔH (kcal·mol^{-1})	11.8 ± 0.8	5.07
$T\Delta S$ (kcal·mol^{-1}deg^{-1})	21.36	13.8
ΔG (kcal·mol^{-1})	−9.56	−8.73

conducted below the phase transition temperature of LPS.[57] Most notably, analyses of ITC data revealed that the native MSI-594 has a higher affinity of interactions ($K_a \approx 13.2\ \mu M^{-1}$) with LPS than the mutant peptide MSI-594F5A ($K_a \approx 3.1\ \mu M^{-1}$) (Table 2).

Conformations of Native MSI-594 and MSI-594F5A in LPS by CD. In aqueous buffer, free native MSI-594 as well as the variant MSI-594F5A showed a strong negative band at ~200 nm, indicating the free peptides adopt unordered conformations (Figure 5A,B, solid lines). In the presence of LPS, both peptides disclose a strong positive band near 192 nm and two negative maxima near 208 nm and ~222 nm, which are reflective of formation of α-helix conformations (Figure 5A,B dotted lines). These observations demonstrate that native MSI-594 and MSI-594F5A have random conformations in free solution; but they show a marked ability to adopt largely α-helical structures in the presence of hydrophobic LPS micelles. NMR studies had previously shown random conformations and helical hairpin structure of MSI-594 in aqueous solution and in the context of LPS micelles, respectively.[33] Further, CD studies indicated that the mutation did not affect the acquisition of the helical secondary structure of the of MSI-594F5A peptide in LPS micelles.

NMR Studies of MSI-594F5A in LPS Micelles. Sequence specific resonance assignments of MSI-594F5A were achieved from combined analyses of 2D $^1H-^1H$ TCOSY and NOESY spectra acquired for the free peptide. The NOESY spectra of the free peptide showed only intra and sequential NOEs, indicating extended or random conformations (data not shown).

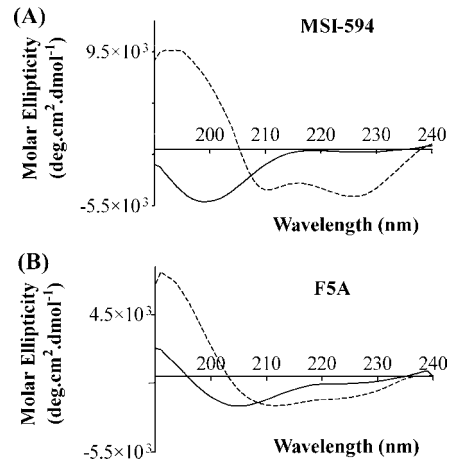

Figure 5. Secondary structures of peptides in free and LPS bound forms by CD spectroscopy. Far-UV CD spectra of native MSI-594 (A), and MSI-594F5A (B), each 25 μM in the absence (solid line) and presence of 50 μM of *E. coli* 0111:B4 LPS (dashed line) in 10 mM sodium phosphate, pH 5.0 at 298 K.

The LPS-bound conformation of MSI-594F5A was investigated by use of tr-NOESY method as described for MSI-594[33] and other LPS interacting peptides.[22,32] tr-NOESY experiments are successful for determining bound conformations of ligands undergoing a fast chemical exchange with the cognate macromolecules.[58−60] NOEs corresponding to the bound state of the ligand are detected at the resonances of the free ligands, as unbound ligands are characterized by few NOE interactions. Intermolecular NOEs between ligand and binding macromolecule are usually not detectable due to significantly lower concentrations of macromolecules used in this experiment.[22,32,33]

As expected, the 2-D $^1H-^1H$ tr-NOESY spectra obtained in presence of LPS micelles, at a peptide:LPS ratio of 20:1, yielded a large number of NOE cross-peaks correlating backbone/backbone and backbone/side chain resonances of MSI-594F5A (Figure 6A,B). Analyses of tr-NOESY spectra of MSI-594F5A revealed the presence of diagnostic medium-range NOEs ($C^\alpha H$ to NH, i to i+2, i+3 and i+4) (Figure 6A), along with sequential NH/NH NOEs for most of the residues (Figure 6B). The pattern of NOE connectivities demonstrates that MSI-594F5A acquires helical conformations in LPS micelles. A close inspection of the per residue NOE distribution indicated that residues Ile2, Ile13, Leu17, Leu20, and Thr21 of MSI-594F5A are characterized by a higher number of NOE contacts in the LPS micelles (Figure 6C). However, at the middle of the sequence residues Lys 10 and Gly 12 appeared to show only sequential NOEs in LPS micelles (Figure 6C). It is noteworthy that in the context of LPS, the mutant peptide MSI-594F5A did not exhibit any detectable long-range NOEs. Several long-range NOE interactions, primarily involving residue Phe5, were observed for the native MSI-594 in LPS micelles defining the helical hairpin structure.[33] The mutated residue Ala5 of MSI-594F5A showed only medium range NOEs akin to helical conformations (Figure 6).

Three-Dimensional Structure of MSI-594F5A in LPS Micelles. The atomic-resolution structure of MSI-594F5A in LPS micelles was determined from 174 tr-NOE driven distance

(57) Bhunia, A.; Domadia, P.; Torres, J.; Hallock, K. J.; Ramamoorthy, A.; Bhattacharjya, S. *J. Biol. Chem.* **2010**, *285*, 3883–3895.
(58) Clore, G. M.; Gronenborn, A. M. *J. Magn. Reson.* **1982**, *48*, 402–417.
(59) Post, C. B. *Curr. Opin. Struct. Biol.* **2003**, *13*, 581–588.
(60) Mayer, B.; Peters, T. *Angew. Chem. Int. Ed.* **2003**, *42*, 865–890.

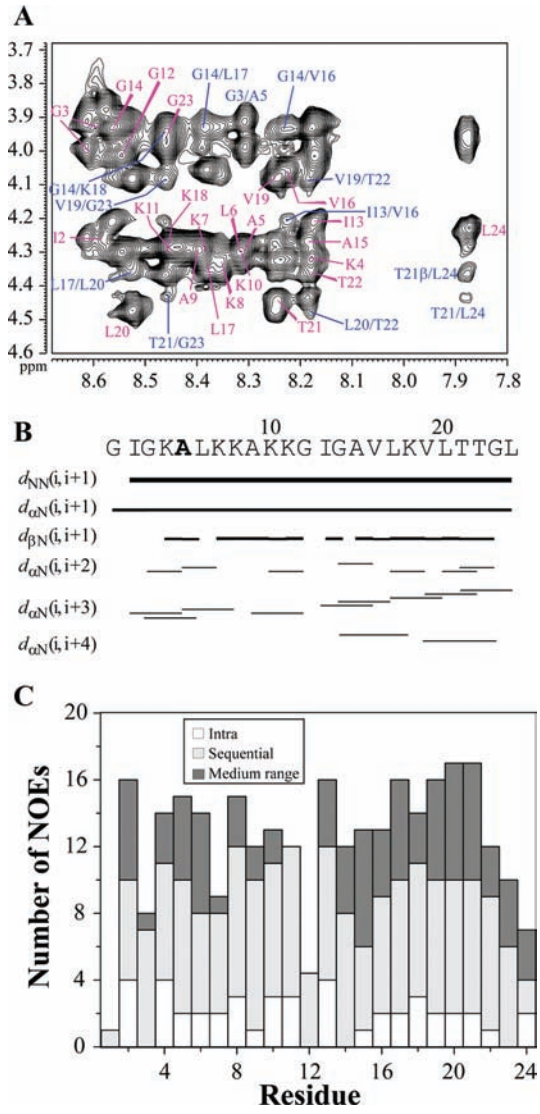

Figure 6. Analyses of tr-NOESY spectra of MSI-594F5A in LPS micelles. (A) $^1H-^1H$ two-dimensional tr-NOESY spectrum of MSI-594F5A showing NOE connectivities in the fingerprint region for NH-C$^\alpha$H resonances. The medium range NOEs are marked in blue, while sequential NOEs are indicated in red. (B) Bar diagram summarizing short-range and medium range NOE contacts, in the tr-NOESY spectra of MSI-594F5A, among backbone/backbone and backbone/side chain resonances. The thickness of the bars indicates the intensity of the NOESY peaks. The primary amino acid sequence of MSI-594F5A is shown at the top. (C) Plot showing number of NOEs observed for MSI-594F5A in complex with LPS micelles as a function of residues. tr-NOESY spectra were obtained in an aqueous solution at peptide:LPS molar ratio of 1:20 at 150 ms mixing time and 298 K.

constraints (Table 3). Figure 7A shows superposition of backbone atoms (N, C$^\alpha$, and C′) of 20 lowest energy structures of MSI-594F5A. The rmsd values for backbone atoms and heavy atoms from the mean conformation were estimated to be 0.72 Å and 1.15 Å, respectively (Table 3). The LPS-bound structure of MSI-594F5A is characterized by a "V" shaped helical structure (Figure 7B). There are two segments, residues I2−K10 and residues I13-T22, of the peptide adopting canonical α-helical conformations in LPS micelles (Figure 7B). The helical conformation turns out to be disrupted at residues K11-G12, whereby G12 assumes nonhelical backbone dihedral angles ($\Phi = -90.5°$, $\Psi = 16.0°$). In the helical hairpin structure of the parent MSI-594 in LPS micelles, these residues were also found to be at the intervening loop connecting two helices.[33] The 3D structures of MSI-594F5A and native MSI-594 in LPS micelles suggest that the central region, at residues K11-G12, of the MSI-594 sequence has an intrinsic tendency to form a loop or bend in the context of outer membrane lipids. The helical hairpin structure of MSI-594 is thus stabilized by interhelical packing involving aromatic side chain of Phe5 with other aliphatic residues (Figure 1). The mutant MSI-594F5A structure in LPS micelles has diminished side chain/side chain packing interactions between the N- and C-termini helices owing to the replacement of aromatic Phe5 to Ala (Figure 7B). In other words, residue Phe5 of MSI-594 appears to be involved in a critical "lock" zipping the two helices into a compact conformation. The curved and open helical structure of MSI-594F5A is predominantly amphipathic in which all of the six positively charged Lys residues are occupying the concave surface of the "V" shaped conformation (Figure 7C). The inner face or the convex side of the structure is rich in nonpolar residues (Figure 7D).

Perturbation of LPS Micelles by MSI-594 and MSI-594F5A. The ability to perturb micelle structure of LPS by AMPs could be correlated with the antimicrobial and antiendotoxic activities.[33,35,57] Dynamic light scattering (DLS) and fluorescence of FITC labeled LPS experiments were carried out to determine structural perturbation of LPS lipids by MSI-594 and MSI-594F5A peptides. Figure 8 shows the DLS measurements of LPS aggregate size in the absence (panel A) and in the presence of MSI-594 (panel B) and MSI-594F5A (panel C) peptides. The hydrodynamic size, in terms of diameter, of LPS aggregates is logarithmically plotted along the *x*-axis. The vertical bars typify the relative percentage of intensity of the LPS particle size distribution. It was observed that in free solution LPS micelles are assembled into larger aggregates showing distribution of sizes up to 6000 nm (Figure 8A). However, in the presence of native MSI-594 peptide, the larger clusters of LPS aggregates, with hydrodynamic diameter more than 500 nm, were observed to be completely absent (Figure 8B). However, in the presence of MSI-594F5A variant, a small population of LPS aggregates having larger sizes of 2000 to 6000 nm are still observed; although most other LPS aggregates illustrated a diameter of less than 500 nm (Figure 8C). The polydispersity index parameter derived from DLS experiments is an indication for the homogeneity of size distribution that may range from values 0 (monodisperse) to 1 (polydisperse). The polydispersity index for free LPS aggregates was estimated to be 0.95, indicating a high degree of polydispersity. As can be seen, LPS aggregates exhibited a drastically reduced polydispersity index of 0.31 in the presence of MSI-594. However, the polydispersity index of LPS solution was observed to be relatively higher, 0.41, in the context of the MSI-594F5A peptide. Thus, MSI-594 bound LPS micelles showed characteristics of monodisperse solution, whereas free LPS solution and MSI-594F5A bound LPS samples were polydisperse in nature. The observed disruption of LPS aggregates to smaller-size particles and a marked change in polydispersity demonstrates the ability of the native MSI-594 peptide to reduce the aggregation state of LPS.

The higher extent of LPS micelle perturbation by the MSI-594 AMP has also been perceived from FITC fluorescence. Upon excitation at 480 nm, soluble aggregates of free FITC-LPS micelles demonstrated very low, self-quenched fluorescence. Further, upon additions of native MSI-594 and variant MSI-594F5A, in increments from nanomolar (100 nm) to micromolar (15 μM) range, a significant enhancement in fluorescence emission intensities of FITC-LPS were conse-

Table 3. A Summary of Structural Statistics for the 20 Final Structures of MSI-594F5A in LPS Micelles

distance restraints	intraresidue ($\|i - j\| = 0$)	45
	sequential ($\|i - j\| = 1$)	83
	medium-range ($2 \leq \|i - j\| \leq 4$)	46
	total	174
angular restraints	(ϕ)	23
distance restraints violations	number of violations	1
	average violations	≤0.29 Å
	maximum violations	≤0.29 Å
deviation from mean structure	all residues (N, C^{α}, C′)	0.72
	heavy atoms	1.15
Ramachandran plot for the mean structure[a]	% residues in the most favorable and additionally allowed region	100
	% residues in the generously allowed region	0
	% residues in the disallowed region	0

[a] Based on PROCHECK-NMR.

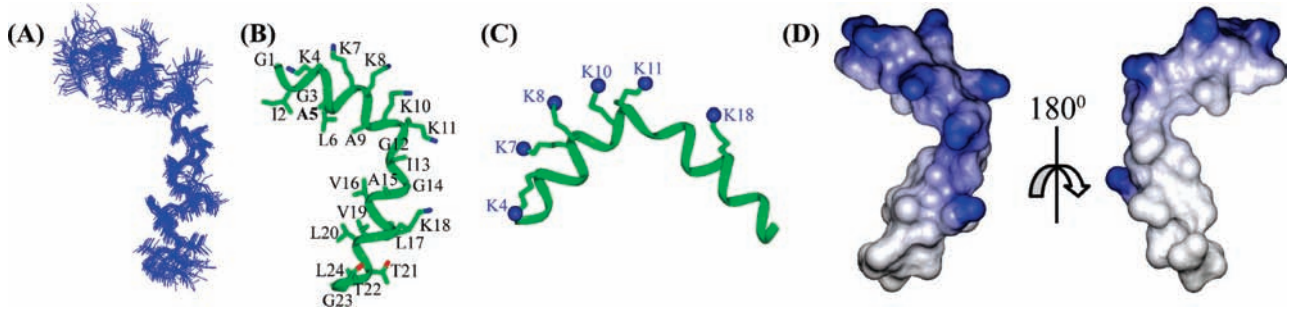

Figure 7. Three-dimensional structure of MSI-594F5A. (A) Superposition of backbone (C^{α}, N, and C′) atoms of the 20 lowest energy structures of MSI-594F5A in LPS micelles. (B) A representative LPS-bound structure of MSI-594F5A showing disposition of cationic and nonpolar residues. The backbone of MSI-594F5A has been depicted as a ribbon. (C) The orientation of the side chain of six basic Lys residues in LPS-bound structure of MSI-594F5A. (D) The electrostatic surface potential of the curved helical structure of MSI-594F5A in the context of LPS micelles.

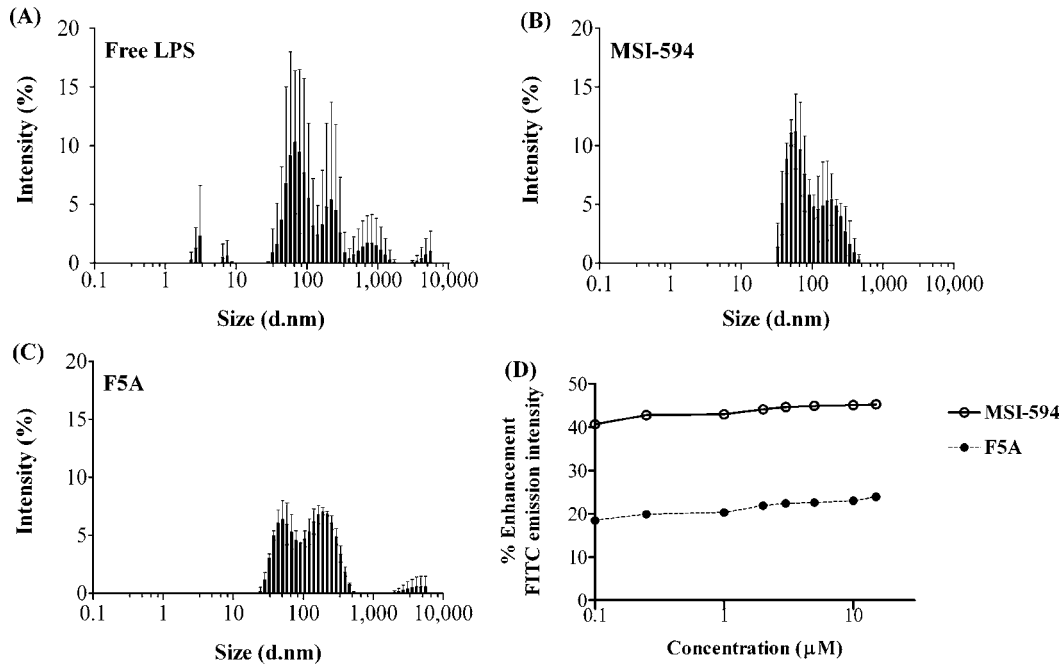

Figure 8. Effects of MSI-594 and MSI-594F5A on LPS micelles. (A) Bar diagrams showing size distribution of LPS particles in free (A) and in presence of peptides, MSI-594 (B) and MSI-594F5A (C) by DLS measurements. DLS experiments were carried out at 1:2 molar ratios of LPS:peptide in 10 mM sodium phosphate, pH 6.0 at 298 K. Standard deviation calculated from 3 runs is shown as error bars. (D) Plot showing enhancement of FITC fluorescence of FITC-labeled LPS with increasing concentrations of MSI-594 and MSI-594F5A peptides. Percentage of fluorescence enhancement observed for 0.5 μM. *E. coli* 055:B5 FITC-LPS as a function of increasing concentrations of peptides (0.1 to 15 μM) in 10 mM sodium phosphate pH 6.0 at 298 K is shown.

quently observed for the native MSI-594 (Figure 8D). At 15 μM, the MSI-594F5A peptide showed only half the dequenching effect as compared to native MSI-594 (Figure 8D). These dequenching effects are observed due to disassembly of FITC-

LPS aggregates, as the distance between its monomers increases upon binding to the peptides. Collectively, these experiments demonstrate that the MSI-594 has a higher ability to bring larger structural changes of LPS micelles as compared to the mutant MSI-594F5A.

Discussion

The LPS layer of the outer membrane plays a vital role in modulating entry and insertion of AMPs to the inner plasma membrane.[6−8] As reported, several AMPs are found to be active against model membranes or bacterial cytoplasmic membranes but rather inactive toward intact bacterial cells.[20,28−31] Insect cecropins, temporins, cathelicidins, protegrins, some defensins are active only against Gram-positive bacteria.[27,31] The outer membrane of Gram-negative bacteria has been attributed to be responsible for inactivation of these AMPs.[28−31] More recent studies, employing designed helical peptides and European frog derived AMPs temporins, have found LPS induced oligomerizations as a leading cause of inactivity of temporins and designed AMPs against Gram-negative bacteria.[28−31] Furthermore, lack of correlations in structure−activity studies of AMPs could potentially arise from inability to cross the LPS layer for cell entry.[28,31] Consequently, the permeability barrier imposed by the outer membrane or polyanionic LPS must be overcome by the broad-spectrum AMPs.[18,20,22] Magainin and its analogues had been shown to induce leakage and create lesions at the outer membrane.[61] The analogues of magainin with higher cationic residues demonstrated higher outer membrane permeabilization activities.[61] IR and CD studies revealed a helical structure of magainin in LPS vesicles and perturbation of acyl chains of lipid A domain of LPS.[61−63] Helical secondary structures for other AMPs in LPS micelles or dispersions were deduced from CD spectroscopy.[64,65] The β-hairpin AMP tachyplesin I, derived from horseshoe crab, adopts LPS-specific structure, determined by its disulfide bridges.[66] The high-affinity interactions of polymyxin B with LPS and plausibly outer membrane permeabilization had been proposed to be dependent on its cyclic structure and N-terminal polyacyl chain.[67−69] However, the mechanisms by which highly active AMPs disrupt the outer membrane LPS layer or limited activities of AMPs conferred by the outer membrane barrier are yet to be fully understood. In this regard, atomic-resolution structures and interactions studies of AMPs in LPS lipids might shed important insights to glean knowledge of outer membrane permeabilization.[22,32,70−72]

MSI-594, obtained from magainin and melittin, is bestowed with potent bactericidal activities with similar low MICs against Gram-negative and Gram-positive bacteria. MSI-594 like many other AMPs of its class, adopts an amphipathic helical structure in phospholipid micelles and bilayers.[44−46] The helical structure has been thought to be responsible for cell lysis destabilizing cytoplasmic membranes via carpet or toroidal pore formations.[44−46] By contrast, a distinctly different structure or a helical hairpin defined by packing of helix−loop−helix, has been realized for MSI-594 in LPS micelles (Figure 1). It would be intriguing to assume that such conformation may be a necessary requirement to disrupt LPS mediated barrier of this broad spectrum AMP.[22,32] In order to determine structure−activity correlation in LPS, the aromatic residue Phe5 of MSI-594, involved in packing between two helices in the hairpin structure has been replaced by Ala yielding a mutant analog MSI-594F5A (Figure 1). In this work, the MSI-594 and MSI-594F5A were compared for their bactericidal activities, outer membrane permeabilization, inner membrane depolarization, LPS binding affinity, and micelles perturbations and secondary structures. The 3-D structure of the mutant MSI-594 F5A peptide determined in the context of LPS micelles helps us to understand the consequence of interhelical interactions in LPS membrane disruption. It is noteworthy that although LPS-bound structure of MSI-594 was described earlier,[33] several other experiments, e.g., NPN uptake, membrane depolarization, interactions with LPS by ITC, DLS, CD, and FITC-LPS fluorescence of MSI-594 have not been previously reported. Our antibacterial assays showed that MSI-594F5A has impaired activities particularly against Gram-negative organisms, suggesting probable inability of the peptide to overcome LPS mediated barrier (Table 1). ANS and NPN uptake experiments had clearly established that F5A mutation has indeed caused restricted ability of the MSI-594F5A to translocate across the outer membrane barrier (Figure 2). However, liposome leakage and EDTA dependent inner membrane depolarization indicated that MSI-594 and MSI594F5A have a similar ability to interact with phospholipid or cytoplasmic membranes of bacteria (Figure 3). ITC measurements showed LPS/MSI peptides interactions are driven by favorable changes in entropy or hydrophobic in nature (Figure 4, Table 2). However, the native MSI-594 binds to LPS micelles with 4-fold higher affinity than the MSI-594F5A mutant (Table 2). Such a high binding affinity of MSI-594 with LPS is further reconciled by disaggregation or destabilization of LPS micelles as deduced from DLS and FITC fluorescence of LPS (Figure 8). The mutant peptide MSI-594F5A exhibited a limited effect toward destabilization of LPS aggregates or micelles (Figure 8). The ability of the MSI-594 to disrupt the outer membrane in NPN and ANS uptake can be correlated with its increased affinity for LPS binding and a larger degree of structural perturbation of LPS aggregates. CD studies delineated structural transitions from random coil to helical conformations in LPS micelles for both of the peptides (Figure 5). However, the NMR structure of MSI-594F5A in LPS micelles has clearly established a disruption of the helical hairpin structure determined for the native peptide (Figure 7). In the context of LPS micelles, MSI-594F5A assumes an amphipathic open type helical structure with significant curvature at the central region (Figures 7B,C). The electrostatic surface potential showed that the outer surface of the bent helical structure is highly basic while the inner surface is nonpolar (Figure 7D). On the basis of functional studies and

(61) Matsuzaki, K.; Sugishita, K.; Harada, M.; Fujii, N.; Miyajima, K. *Biochim. Biophys. Acta* **1997**, *1327*, 119–130.
(62) Rana, F. R.; Macias, E. A.; Sultany, C. M.; Modzrakowski, M. C.; Blazyk, J. *Biochemistry* **1991**, *30*, 5858–5866.
(63) Matsuzaki, K.; Sugishita, K.; Miyajima, K. *FEBS Lett.* **1999**, *449*, 221–224.
(64) Tack, B. F.; Sawai, M. V.; Kearney, W. R.; Robertson, A. D.; Sherman, M. A.; Wang, W.; Hong, T.; Boo, L. M.; Wu, H.; Waring, A. J.; Lehrer, R. I. *Eur. J. Biochem.* **2002**, *269*, 1181–1189.
(65) Chen, C.; Brock, R.; Luh, F.; Chou, P. J.; Larrick, J. W.; Huang, R. F.; Huang, T. H. *FEBS Lett.* **1995**, *370*, 46–52.
(66) Hirakura, Y.; Kobayashi, S.; Matsuzaki, K. *Biochim. Biophys. Acta* **2002**, *1562*, 32–36.
(67) Bhattacharjya, S.; David, S. A.; Mathan, V. I.; Balaram, P. *Biopolymers* **1997**, *41*, 251–265.
(68) Pristovsek, P.; Kidric, J. *J.Med.Chem.* **1999**, *42*, 4604–4613.
(69) Velkov, T.; Thompson, P. E.; Nation, R. L.; Li, J. *J. Med. Chem.* **2010**, *53*, 1898–1916.
(70) Bhunia, A.; Domadia, P. N.; Bhattacharjya, S. *Biochim. Biophys. Acta* **2007**, *1768*, 3282–3291.
(71) Bhunia, A.; Chua, G. L.; Domadia, P. N.; Warshakoon, H.; Cromer, J. R.; David, S. A.; Bhattacharjya, S. *Biochem. Biophys. Res. Commun.* **2008**, *369*, 853–857.
(72) Bhunia, A.; Mohanram, H.; Bhattacharjya, S. *Biopolymers* **2009**, *92*, 9–22.

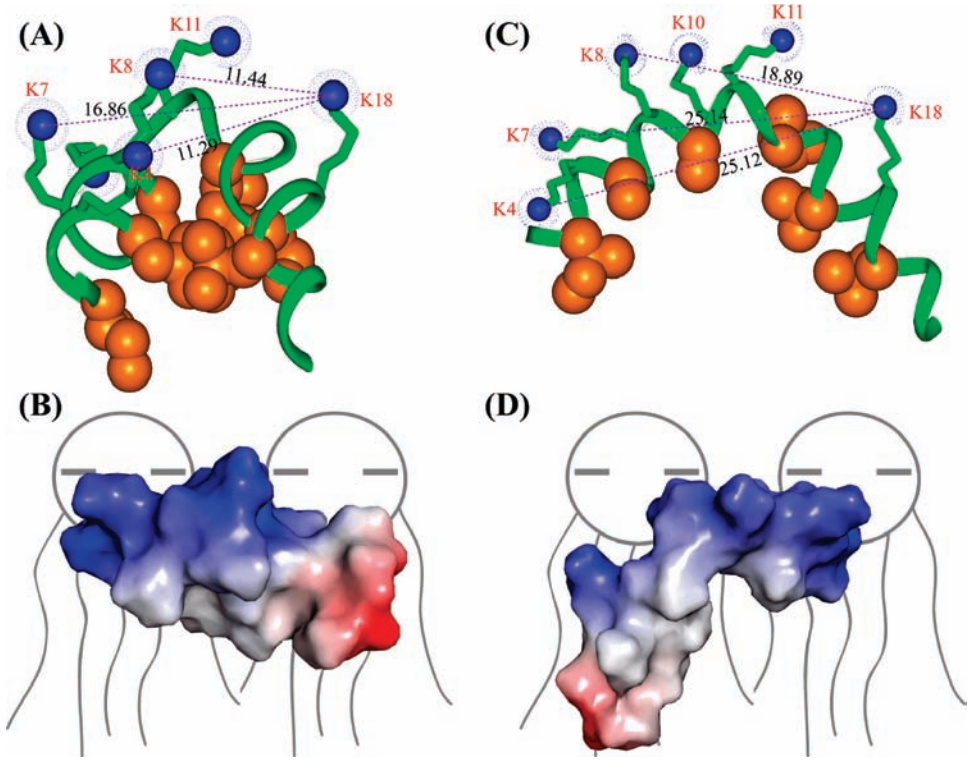

Figure 9. Mode of interactions of MSI-594 and MSI-594F5A with LPS layer. (A) Distribution of cationic and hydrophobic residues of MSI-594 in the helical hairpin structure determined in LPS micelles. The distances between the nitrogen atoms of the side chain $N^{\epsilon}H_3^+$ groups are indicated. (B) A model of interaction between LPS layer and MSI-594 showing basic charge residues are congregated for plausible high-affinity interactions with the negatively charged phosphate groups of LPS layer. (C) Distribution of cationic and hydrophobic residues of MSI-594F5A peptide in curved helical structure determined in LPS micelles. The distances between the nitrogen atoms of the side chain $N^{\epsilon}H_3^+$ groups are indicated. (D) A model of interaction between LPS layer and MSI-594F5A showing scattered basic charges in the open helical structure may cause a reduced cell wall permeabilization.

LPS binding affinity, the curved structure of the mutant MSI-594, although amphipathic, demonstrated to possess a restricted ability to premeablize the outer membrane compared to the native peptide. Analysis of the hairpin structure of the MSI-594 and open helical structure of the mutant MSI-594F5A provides mechanistic insights into the superior activity of the native peptide to disrupt outer membrane integrity. The helical hairpin structure of MSI-594 displays several of the cationic side chains of Lys residues in a compatible geometrical arrangement to the interphosphate distance (∼13−14 Å) of lipid A moiety of LPS (Figure 9A). In particular, in the helical hairpin structure of MSI-594 side chains H_3N^+ groups of Lys4/Lys18 and Lys7/Lys18 across the two helices are constrained to interact favorably, salt-bridges or H-bonds, with the two phosphate groups of lipid A (Figure 9A). Furthermore, in the helical hairpin structure of MSI-594, all of the side chains of basic Lys residues are pointed along the same direction, creating a uniform surface of cationic charges of high density (Figure 9B). Such disposition of a positively charged surface rendered by the helical hairpin structure of MSI-594 might lead to a facile permeabilization of the outer membrane (Figure 9B). These structural features are largely absent in the LPS-bound structure of the mutated MSI-594F5A (Figure 9C). In the noncompact helical structure, the positively charged residues are spread over whereby side chains of Lys4/Lys18 and Lys7/Lys18 are no longer in appropriate proximity with the interphosphate distance of lipid A of LPS (Figure 9C). By contrast to the native MSI-594, the LPS-bound structure of MSI-594F5A also displays a diffused distribution of basic surface charges over its curved helical structure that may reduce the ability of the mutant peptide to permeabilize the outer membrane barrier (Figure 9D). The electrostatic interactions have been known to play dominant roles in binding between cationic AMPs and the highly negatively charged LPS layer of the outer membrane.[9,10,13] Furthermore, a retarded or slow translocation efficiency of the mutant peptide MSI-594F5A may occur as a result of an extended or open helical structure exposing most of the hydrophobic residues (Figure 9). Further, the exposed nonpolar residues may induce intermolecular aggregations or become trapped as a consequence of interactions with LPS molecules.

As such, the current work demonstrated a correlation between the structure of a potent AMP in LPS with the outer membrane permeabilization activity. However, a significant number of studies have suggested that structure−function relationships in AMPs are rather poorly defined.[73−79] Most notably, incorporation of D-amino acids into the sequences of either helical or β-sheet AMPs had been observed to destabilize conformations while retaining much of the antibacterial activities.[73−76,80] More recent studies utilizing short β-sheet AMPs, screened from a combinatorial library, delineated a lack of strong correlations

(73) Oren, Z.; Hong, J.; Shai, Y. *J. Biol. Chem.* **1997**, *272*, 14643–14649.
(74) Oren, Z.; Shai, Y. *Biochemistry* **1997**, *36*, 1826–1835.
(75) Kondejewski, L. H.; Jelokhani-Niaraki, M.; Farmer, S. W.; Lix, B.; Kay, C. M.; Sykes, B. D.; Hancock, R. E.; Hodges, R. S. *J. Biol. Chem.* **1999**, *274*, 13181–13192.
(76) Lee, D. L.; Hodges, R. S. *Biopolymers* **2003**, *71*, 28–48.
(77) Rathinakumar, R.; Wimley, W. C. *J. Am. Chem. Soc.* **2008**, *130*, 9849–9858.
(78) Rathinakumar, R.; Walkenhorst, W. F.; Wimley, W. C. *J. Am. Chem. Soc.* **2009**, *131*, 7609–7617.
(79) Porter, E. A.; Weisblum, B.; Gellman, S. H. *J. Am. Chem. Soc.* **2005**, *127*, 11516–11529.
(80) Saravanan, R.; Bhunia, A.; Bhattacharjya, S. *Biochim. Biophys. Acta* **2010**, *1798*, 128–139.

between conformations and antibacterial activities.[77,78] However, these studies had found that structural destabilization appeared to be detrimental toward the broad spectrum activities of AMPs.[77,78] Designed antimicrobial peptides containing non-natural β-amino acids had shown an increase in helical content does not lead to a higher microbial sterilization.[79] Collectively, it has been postulated that the antimicrobial activities of AMPs are largely governed by the optimized sequences, rather than by specific structures, typified by a balanced amphipathicity, solubility, and ability to disrupt membrane integrity. By contrast, rational engineering starting from an existing scaffold of AMPs has also yielded potent analogs with superior activities as compared to the parent peptides.[81−83] We surmise that structure−activity relationships of AMPs could be highly context dependent, whereby specific structures might be stabilized at various targets including outer membranes, plasma membrane, or intracellular components of microbes. It is also noteworthy that low resolution structural methods like CD are frequently being used in structure−activity studies. As shown here and elsewhere, active AMPs assume higher order secondary structures with packing interactions in the LPS or outer membrane.[33,35,53,84] Such intrapeptide packing interactions are demonstrated to play critical roles[35,57] and should be considered in order to elucidate structure−activity correlations of AMPs.

Conclusions

The structural basis of outer membrane or LPS permeabilization by antimicrobial peptides is not clearly understood. MSI-594 represents a highly active broad-spectrum helical antimicrobial peptide that acquires a compact helical hairpin structure in complex with LPS. Using a battery of methods including functional, biophysical, and NMR, this work demonstrated that potent AMPs, like MSI-594, may be acquiring specific structure in the context of outer membrane lipid or LPS in order to disrupt the outer membrane barrier of Gram-negative organisms. We propose that atomic-resolution structures of AMPs in LPS and correlations with activities would aid in the development of potent antimicrobial and antiendotoxic compounds.

Acknowledgment. The work was supported in part by research Grants 06/1/22/19/446 and 08/1/22/19/556 from A*BMRC, Singapore (to S.B.), and was partly supported by the National Institutes of Health (GM084018 to A.R.). The atomic coordinates of MSI-594F5A structures have been deposited to the Protein Data Bank under the accession number: 2L36.

JA1083255

(81) Won, H. S.; Jung, S. J.; Kim, H. E.; Seo, M. D.; Lee, B. J. *J. Biol. Chem.* **2004**, *279*, 14784–14791.
(82) Blazyk, J.; Wiegand, R.; Klein, J.; Hammer, J.; Epand, R. M.; Epand, R. F.; Maloy, W. L.; Kari, U. P. *J. Biol. Chem.* **2001**, *276*, 27899–27906.
(83) Tossi, A.; Sandri, L.; Giangaspero, A. *Biopolymers* **2000**, *55*, 4–30.
(84) Bhattacharjya, S.; Domadia, P. N.; Bhunia, A.; Malladi, S.; David, S. A. *Biochemistry* **2007**, *46*, 5864–5874.